Astron. Astrophys. 339, 261–271 (1998)

ASTRONOMY AND ASTROPHYSICS

Are solar granules the only source of acoustic oscillations?

T. Foglizzo

Service d'Astrophysique, CEA/DSM/DAPNIA, CE-Saclay, F-91191 Gif-sur-Yvette, France

Received 27 July 1998 / Accepted 27 August 1998

Abstract. The excitation mechanism of low degree acoustic modes is investigated through the analysis of the stochastic time variations of their energy. The correlation between the energies of two different modes is interpreted as the signature of the occurrence rate of their excitation source. The different correlations determined by Foglizzo et al. (1998) constrain the physical properties of an hypothetical source of excitation, which would act in addition to the classical excitation by the turbulent convection. Particular attention is drawn to the effect of coronal mass ejections. The variability of their occurrence rate with the solar cycle could account for the variation of the correlation between IPHIR and GOLF data. Such an interpretation would suggest that the mean correlation between low degree acoustic modes is at least 0.2% at solar minimum.

Key words: Sun: oscillations – Sun: activity – Sun: flares – Sun: granulation – methods: statistical

1. Introduction

The theoretical mechanism of excitation of solar acoustic modes by the turbulent convection is well documented (Goldreich & Keeley 1977; Goldreich & Kumar 1988; Kumar & Goldreich 1989; Balmforth 1992a,b,c; Goldreich et al. 1994). High frequency oscillations were interpreted in different ways (Kumar & Lu 1991; Goode et al. 1992; Restaino et al. 1993; Vorontsov et al. 1998), in order to address the question of the depth of the excitation source. Local observations led Rimmele et al. (1995) and Espagnet et al. (1996) to identify the excitation of 5-minute oscillations with acoustic events occurring in the downflowing intergranular regions, rather than overshooting granules.

Considering granules of 1000 km diameter renewed on a time scale comparable with their turnover time (8 min), there are about 5×10^9 excitations by solar granules per damping time (3.7 days). Even if the number of efficient excitations is smaller by a factor 100 (Brown 1991), each low degree mode is stochastically excited so many times per damping time, that modes with different frequencies are expected to have uncorrelated energies. In particular, the fitting procedures used to determine the frequency, linewidth, and splitting of p modes often rely on the statistical independence of neighbouring modes (e.g. Appourchaux et al. 1998).

Baudin et al. (1996), however, noticed a possible correlation between low degree p modes in IPHIR data. By measuring the mean correlation of p modes in IPHIR and GOLF data, and determining their statistical significance, Foglizzo et al. (1998) (hereafter F98) suggested the existence of an additional source of excitation during the IPHIR period (end of 1988).

The goal of this study is to use the observed correlations as a constraint on the physical properties of this hypothetical additional source. The theoretical relationship between the occurrence rate of this source, its contribution to the energy of low degree p modes, and their correlation coefficient, is established in Sect. 2. Available observational constraints are reviewed in Sect. 3. The possible role of comets, X-ray flares and coronal mass ejections (CMEs) is discussed in Sect. 4.

Send offprint requests to: foglizzo@cea.fr

2. Correlation coefficient between two modes excited by a single mechanism

2.1. The energy of a mode seen as a random walk

Let us consider impulsive excitations, distributed over the solar surface. The exciting events, indexed by k, occur at the random poissonian time t_k. They correspond to a radial velocity perturbation $v_k(\mathbf{r})$ localized in a cone of angle α_k around the random direction (θ_k, ϕ_k), with a radial extension δr_k. $v_k(\mathbf{r})$ is described by an amplitude v_k and dimensionless shape functions g_k and h_k as follows:

$$v_k(\mathbf{r}) \equiv g_k(\alpha) h_k(r) v_k, \tag{1}$$

$$h_k(r) \sim 1 \text{ for } R_\star > r > R_\star - \delta r_k, \tag{2}$$

$$g_k(\alpha) \sim 1 \text{ for } \alpha < \alpha_k. \tag{3}$$

$\alpha(\theta, \theta_k, \phi - \phi_k) \geq 0$ is the angle made by the direction θ, ϕ with the direction θ_k, ϕ_k. Let M_k be the mass of gas in the volume defined by the functions g_k and h_k, so that the kinetic energy of the perturbation is $\mathcal{E}_k = M_k v_k^2/2$. The mean interpulse time is defined as $\Delta t \equiv < t_{k+1} - t_k >$.

We assume that each impulsive event triggers free oscillations of the set of p modes. Each perturbation is projected onto the basis of eigenvectors. The damping time τ_d depends in principle on the mode considered, but is nearly constant ($\sim$ 3.7 days)

for the modes considered by F98, in the plateau region between 2.5mHz and 3.5mHz (linewidth of 1μHz).
In appendix A it is shown that the total energy of the oscillations associated to the frequency $\omega_{nl}+m\Omega$ is:

$$E^+_{nlm}(t) \;=\; \left|\sum_{t_k<t} \mathrm{e}^{-\frac{t-t_k}{\tau_d}} a^k_{nlm} \mathrm{e}^{i\Phi^k_{nlm}}\right|^2, \tag{4}$$

$$a^k_{nlm} \;\equiv\; g^k_{lm}(\theta_k) h^k_{nl} M_k^{\frac{1}{2}} v_k, \tag{5}$$

$$\Phi^k_{nlm} \;\equiv\; (\omega_{nl}+m\Omega)t_k + m\phi_k. \tag{6}$$

where the real function $g^k_{l,m}=g^k_{l,-m}$ depends on the angular shape of the excitation projected onto the spherical harmonics, and h^k_{nl} depends on the radial shape of the excitation projected onto the radial part $v^r_{nl}(r)$ of the eigenfunction:

$$g^k_{lm}(\theta_k) \;\equiv\; q_{lm}\int_0^{\frac{\alpha_k}{2}} \mathrm{d}\phi \int_0^{\pi} \mathrm{d}(\cos\theta) P_l^{|m|}(\cos\theta) \times\; \cos(m\phi) g_k(\theta,\theta_k,\phi), \tag{7}$$

$$h^k_{nl} \;\equiv\; \frac{1}{M_k^{\frac{1}{2}}}\int_{R_\star-\delta r_k}^{R_\star} \rho r^2 v^r_{nl}(r) h_k(r) \mathrm{d}r. \tag{8}$$

The relationship between the spherical harmonics and the Legendre associated functions P_l^m through the constant q_{lm} is recalled in Eqs. (A5)-(A6). The exponential damping in Eq. (4) can be schematized as a term selecting the finite set of excitations which occurred within one damping time before the time t:

$$E^+_{nlm}(t) \sim \left|\sum_{0<t-t_k<\tau_d} a^k_{nlm} \mathrm{e}^{i\Phi^k_{nlm}}\right|^2. \tag{9}$$

The series of phases $\omega_{nl}t_k$ and ϕ_k are independent random variables uniformly distributed in the interval $[0,2\pi]$. The series Φ^k_{nlm} defined by Eq. (6) is therefore also uniformly distributed in $[0,2\pi]$. Ignoring the academic case where the ratio of the frequencies is a simple rational number, Φ^k_{nlm} and $\Phi^k_{n'l'm'}$ can be considered independent for two different realistic modes.
As a consequence, the energy of the wave is interpreted as the squared length of a random walk in the complex plane. Each step of this random walk is defined by an amplitude a^k_{nlm}, and a phase Φ^k_{nlm} (negative values of the amplitude can be converted into an increment of the phase). The number of steps N is the number of excitations, over the whole surface of the sun, within one damping time:

$$N \equiv \frac{\tau_d}{\Delta t}. \tag{10}$$

The central limit theorem ensures that the real and imaginary parts of the complex sum (9) converge towards independent normal distributions if N is large enough, resulting in an exponential distribution of energy (see also Kumar et al. 1988).
According to this random walk interpretation, two different modes excited by the same series of events must have correlated energies. This correlation should approach 100% if the number of steps of this random walk is small, i.e. if the interpulse mean time Δt is longer than the damping time τ_d.
The independence of the phases Φ^k_{nlm} and $\Phi^k_{n'l'm'}$, however, makes the correlation decrease to zero when the number of excitations increases.
In particular, the random walks associated with the two components $\omega_{nl}\pm m\Omega$ of a mode n,l have the same series of amplitudes, but have two independent series of phases. This leads us to expect that waves travelling in opposite directions do not have the same instantaneous total energy (except on average), although they are excited by the same events.

2.2. Theoretical correlation between the energies of two modes

The mean energy $<E_{nlm}>$ of the mode nlm is directly proportional to the mean energy $<e_{nlm}>$ received from each excitation (appendix B):

$$<E_{nlm}> = \frac{N}{2} <e_{nlm}>. \tag{11}$$

The correlation $\mathcal{C}^{n'l'm'}_{nlm}$ between two modes $nlm, n'l'm'$ excited by the same source described by Eq. (4) is derived in appendix B:

$$\mathcal{C}^{n'l'm'}_{nlm} = \frac{<e_{nlm}e_{n'l'm'}>}{<e^2_{nlm}>^{\frac{1}{2}}<e^2_{n'l'm'}>^{\frac{1}{2}}} \times \left(1+N\frac{<e_{nlm}>^2}{<e^2_{nlm}>}\right)^{-\frac{1}{2}} \left(1+N\frac{<e_{n'l'm'}>^2}{<e^2_{n'l'm'}>}\right)^{-\frac{1}{2}}. \tag{12}$$

2.3. Latitudinal distribution and sizes of the excitations

The ratio $<e^2_{nlm}>/<e_{nlm}>^2$, related to the spread of the distribution, is called kurtosis (it is sometimes defined with an additional constant -3 which we omit here).

$$\frac{<e^2_{nlm}>}{<e_{nlm}>^2} = \frac{<g^4_{lm}h^4_{nl}\mathcal{E}^2>}{<g^2_{lm}h^2_{nl}\mathcal{E}>^2}. \tag{13}$$

The kurtosis of e_{nlm} is partly produced by the kurtosis of $\mathcal{E}_k$ (independent of nlm), but also by the projection of the spatial distribution of excitations $(\theta_k,\alpha_k,\delta r_k)$ onto the eigenfunctions nlm.
The random variations of the size $\alpha_k,\delta r_k$ of the excitation play a negligible role as long as it is smaller than the wavelength of the mode nlm. For the modes $l=0$ and $l=1$ analysed by F98, we restrict ourselves to perturbations such that $\alpha_k<\pi$, and δr_k is smaller than the depth of the first radial node of the eigenfunction v_{nl}, and thus neglect the random variations of $\alpha_k,\delta r_k$.
Let us estimate the kurtosis of the distribution $g_{lm}(\theta_k)$, due to the projection of the latitudinal distribution of excitations on the mode nlm. From Eq. (7), the function $g_{lm}(\theta_k)$ is independent of θ_k for the radial mode $l=0$:

$$\frac{<g^4_{0,0}>}{<g^2_{0,0}>^2} = 1. \tag{14}$$

By contrast, the mode $l = 1, m = \pm 1$ is more excited by equatorial events than polar ones. For small scale excitations ($\alpha_k \equiv 0$) distributed uniformly over the sphere, Eq. (7) implies:

$$\frac{< g_{1,\pm1}^4 >}{< g_{1,\pm1}^2 >^2} = \frac{6}{5}. \tag{15}$$

The kurtosis of $g_{1,\pm1}^2$ should reach a value even closer to unity if the excitations are distributed in an equatorial region, like CMEs at solar minimum or big flares.

Let us approximate the kurtosis of e_{nlm} as the product of the kurtosis of $\mathcal{E}_k$ by the kurtosis of $g_{lm}^2(\theta_k)$.

$$\frac{< e_{nlm}^2 >}{< e_{nlm} >^2} \sim \frac{< \mathcal{E}^2 >}{< \mathcal{E} >^2} \times \frac{< g_{lm}^4 >}{< g_{lm}^2 >^2}. \tag{16}$$

Using this approximation in Eq. (12), the correlation between low degree modes $l = 0, m = 0$ and $l = 1, m = \pm 1$ excited in the random direction (θ_k, ϕ_k) by a small scale excitation ($\alpha_k \equiv 0$) is:

$$\mathcal{C}_{n,0,0}^{n',0,0} = (1 + N_{\rm eff})^{-1}, \tag{17}$$

$$\mathcal{C}_{n,0,0}^{n',1,\pm1} = \left(\frac{5}{6}\right)^{\frac{1}{2}} (1 + N_{\rm eff})^{-\frac{1}{2}} \left(1 + \frac{5N_{\rm eff}}{6}\right)^{-\frac{1}{2}}, \tag{18}$$

$$\mathcal{C}_{n,1,\pm1}^{n',1,\pm1} = \left(1 + \frac{5N_{\rm eff}}{6}\right)^{-1}, \tag{19}$$

where we have incorporated the kurtosis of $\mathcal{E}_k$ into the definition of the effective number $N_{\rm eff}$ of excitations per damping time:

$$\beta \equiv \frac{< \mathcal{E}^2 >}{< \mathcal{E} >^2} \geq 1, \tag{20}$$

$$N_{\rm eff} \equiv \frac{N}{\beta}. \tag{21}$$

The correlation displayed in Fig. 1 appears to be hardly sensitive to the geometrical content of the function g_{lm}, since all curves are similar within 10%. Error bars of the observationally measured correlations being typically larger than 0.1, Eq. (17) shall be considered accurate enough for the purpose of this study:

$$\mathcal{C}_{n,l,m}^{n',l',m'} \sim (1 + N_{\rm eff})^{-1}. \tag{22}$$

This is equivalent to approximating the kurtosis of e_{nlm} by the kurtosis of $\mathcal{E}$.

2.4. Case of two excitation mechanisms superimposed

F98 used a one parameter model of two sources of excitation, such that each mode contains a fraction λ of energy common to all the modes. They assumed that both sources produce exponential distributions of energy. This simplification led to the simple relation $\lambda = \mathcal{C}^{1/2}$. This simplification, however, does not apply to the case of a correlation produced by rare impulsive events. If $N \ll 1$, the energy is damped to zero except during isolated pulses of duration $\sim \tau_{\rm d}/2$. The distribution E thus follows a Bernoulli statistics, with $\mathrm{Var}(E)/ < E >^2 \gg 1$ (Eq. B8) instead of 1 for an exponential distribution. The occurrence rate of the excitation mechanism therefore appears to be a key parameter which cannot be neglected. Let us consider two excitations mechanisms acting simultaneously on two modes n, l, m and n', l', m':

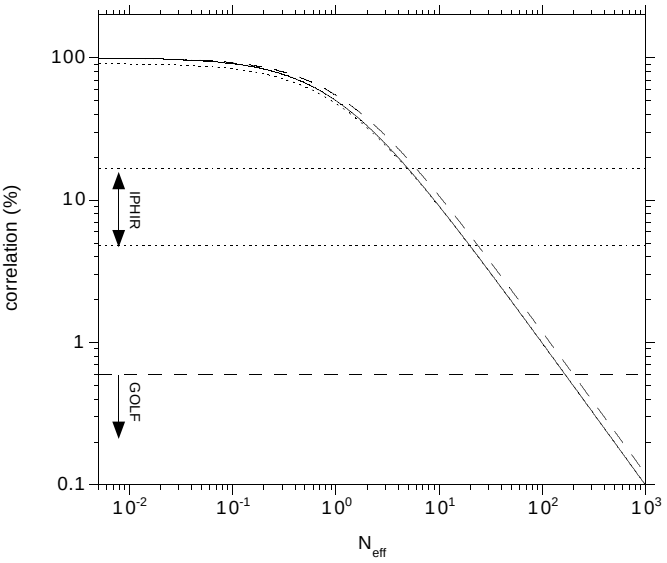

Fig. 1. Theoretical correlation between two modes $l = 0$ (full line), $l = 0$ and $l = 1, m = 1$ (dotted line), and $l = 1, m = \pm 1$ (dashed line), as a function of the number of effective excitations per damping time ($\alpha_k \equiv 0$). Horizontal lines indicate the measured correlation in IPHIR data and the upper bound found in GOLF data.

(i) excitation by granules, with a high occurrence rate ($N_1 \gg 1$).

(ii) excitation by additional events with a total acoustic energy $\mathcal{E}_{\rm ad}^k$, occurring on average $N_{\rm ad}$ times per damping time, and contributing to a fraction λ_{nlm} of the power of the mode nlm.

We show in appendix C (Eq. C7) that the correlation between the energies of two oscillators excited by these sources is the same as in Eq. (12), but multiplying the kurtosis of e_{nlm} by λ_{nlm}^2. The latitudinal distribution and sizes of the excitations play a relatively small role according to Sect. 2.3. The effective number $N_{\rm eff}$ of excitations per damping time depends on the kurtosis $\beta_{\rm ad}$ of $\mathcal{E}_{\rm ad}$:

$$N_{\rm eff} \equiv \frac{N_{\rm ad}}{\beta_{\rm ad}}. \tag{23}$$

Making the additional assumption that the fraction $\lambda_{nlm} = \lambda$ varies little among the modes considered by F98. The mean correlation between these modes is:

$$\mathcal{C} \sim \left(1 + \frac{N_{\rm eff}}{\lambda^2}\right)^{-1}. \tag{24}$$

A significant correlation can thus be produced by a source representing only a small fraction λ of the total power of each mode if $N_{\rm eff}$ is small enough.

Interpreting the observed correlation $\mathcal{C}$ as a consequence of an

additional source of excitation therefore requires it to contribute to a fraction λ of the total power, deduced from Eq. (24):

$$\lambda \sim \left\{ \frac{\mathcal{C}\ N_{\rm eff}}{1-\mathcal{C}} \right\}^{\frac{1}{2}} . \tag{25}$$

According to Eq. (11), the fraction λ of power coming from the additional source is related to the mean acoustic energy input $< e_{\rm ad} >$ into the mode nlm:

$$\lambda = \frac{N_{\rm ad}}{2} \frac{< e_{\rm ad} >}{< E >}. \tag{26}$$

Eq. (25) becomes:

$$< e_{\rm ad} > \ = \ \frac{2}{\beta_{\rm ad}} \frac{\mathcal{C}}{1-\mathcal{C}} \frac{< E >}{\lambda}, \tag{27}$$

$$= \ \frac{2}{\beta_{\rm ad}^{\frac{1}{2}}} \left\{ \frac{\mathcal{C}}{1-\mathcal{C}} \right\}^{\frac{1}{2}} \frac{< E >}{N_{\rm ad}^{\frac{1}{2}}}. \tag{28}$$

Let us assume that the occurrence rate $N_{\rm ad}$ varies from $N_{\rm min}$ to $N_{\rm max}$ with the solar cycle, while the properties of the exciting events ($< e_{\rm ad} >, \beta_{\rm ad}$) remain unchanged. We use Eq. (28) to express the relationship between the minimum and maximum correlations $\mathcal{C}_{\rm min}, \mathcal{C}_{\rm max}$:

$$\mathcal{C}_{\rm min} = \left\{ 1 + \frac{N_{\rm max}}{N_{\rm min}} \frac{1-\mathcal{C}_{\rm max}}{\mathcal{C}_{\rm max}} \left(\frac{< E >_{\rm min}}{< E >_{\rm max}} \right)^2 \right\}^{-1}. \tag{29}$$

2.5. Efficiency of the generation of acoustic waves

Since the distribution of acoustic energy $\mathcal{E}_{\rm ad}$ produced by the additional source is not directly observable, we are led to assume that it resembles the observed distribution of total energy $\mathcal{E}_{\rm T}$ of the additional source. Let $p_{\rm T}(\mathcal{E})$ be the density of probability of the source of energy $\mathcal{E}_{\rm min} \leq \mathcal{E}_{\rm T} \leq \mathcal{E}_{\rm max}$, occurring $N_{\rm T}$ times per damping time. Let us assume that the excitation of low degree modes is efficient only in the range $\mathcal{E}_1 \leq \mathcal{E}_{\rm T} \leq \mathcal{E}_2$, inside which the efficiency $f_{\rm ad} \equiv \mathcal{E}_{\rm ad}/\mathcal{E}_{\rm T}$ is constant:

$$\mathcal{E}_{\rm ad} \ = \ f_{\rm ad} \mathcal{E}_{\rm T} \ \ \text{for} \ \mathcal{E}_1 \leq \mathcal{E}_{\rm T} \leq \mathcal{E}_2, \tag{30}$$

$$\mathcal{E}_{\rm ad} \ = \ 0 \ \ \text{otherwise}. \tag{31}$$

In appendix C, Eq. (28) is rewritten as the fraction of the mean acoustic energy $< \mathcal{E}_{\rm ad} >$ which must be injected into each mode nlm in order to produce the observed correlation:

$$\frac{< e_{\rm ad} >}{< \mathcal{E}_{\rm ad} >} =$$

$$\frac{2}{f_{\rm ad} \left(\int_{\mathcal{E}_1}^{\mathcal{E}_2} \mathcal{E}^2 p_{\rm T}(\mathcal{E}) {\rm d}\mathcal{E} \right)^{\frac{1}{2}}} \left\{ \frac{\mathcal{C}}{1-\mathcal{C}} \right\}^{\frac{1}{2}} \frac{< E >}{N_{\rm T}^{\frac{1}{2}}}. \tag{32}$$

This fraction is therefore minimal when the range of efficient excitations $\mathcal{E}_1, \mathcal{E}_2$ contains the range of energies where the product $\mathcal{E}_{\rm T}^2 p(\mathcal{E}_{\rm T})$ is maximal. Using in Eq. (28) the occurrence rate $N_{\rm T}$ and kurtosis $\beta_{\rm T}$ of the distribution of total energy $\mathcal{E}_{\rm T}$ instead of the distribution of acoustic energy $\mathcal{E}_{\rm ad}$ leads to a lower bound of the ratio $< e_{\rm ad} > / < \mathcal{E}_{\rm ad} >$:

$$\frac{< e_{\rm ad} >}{< \mathcal{E}_{\rm ad} >} \geq \frac{1}{f_{\rm ad}} \frac{2}{N_{\rm T}^{\frac{1}{2}} \beta_{\rm T}^{\frac{1}{2}}} \left\{ \frac{\mathcal{C}}{1-\mathcal{C}} \right\}^{\frac{1}{2}} \frac{< E >}{< \mathcal{E}_{\rm T} >}. \tag{33}$$

For a given excitation mechanism one can estimate the number $\mathcal{N}$ of p modes with a wavelength longer than the size of each exciting event, which receive a comparable amount of energy from the source. Considering that the low degree modes in F98 belong to this set,

$$< \mathcal{E}_{\rm ad} > = \sum_{nlm} < e_{nlm} > \geq \mathcal{N} < e_{\rm ad} > . \tag{34}$$

From Eqs. (33)-(34) we deduce a constraint on observable quantities, which shall be useful in Sect. 4 in order to discriminate between possible excitation mechanisms:

$$\frac{2}{N_{\rm T}^{\frac{1}{2}} \beta_{\rm T}^{\frac{1}{2}}} \left\{ \frac{\mathcal{C}}{1-\mathcal{C}} \right\}^{\frac{1}{2}} \frac{< E >}{< \mathcal{E}_{\rm T} >} \leq \frac{f_{\rm ad}}{\mathcal{N}} < \frac{1}{\mathcal{N}}. \tag{35}$$

3. Observational constraints

3.1. Exponential distribution of individual p modes energy

The distribution of energy of low degree p modes agrees reasonably well with an exponential distribution (Chaplin et al. 1995, 1997 for BiSON data, F98 for IPHIR and GOLF data). Chaplin et al. (1995, 1997), however, noticed significant deviations in the high energy tail of the distribution, which could be due to an additional excitation mechanism. They estimated that the probability that such deviations occur by chance during the period of observation is only 0.1%. Among 22512 events covering 18331 hours of BiSON data from 1987 to 1994, Chaplin et al. (1997) found 51 events above 6.5 times the mean energy, whereas less than 41 would be expected in 90% of the cases for an exponential distribution. Crudely speaking, about 10 events are unexpected in the distribution, suggesting $N_{\rm ad} \geq 0.05$.

3.2. Solar cycle variations of the total power of low degree p modes

The typical energy of a low degree p mode in the range $2.7{\rm mHz} \leq \nu \leq 3.4{\rm mHz}$ considered by F98 is $< E > \sim 8 \times 10^{27}$ ergs (Chaplin et al. 1998). The velocity damping time being $\tau_d \sim 3.7$ days, the flux of energy required to excite this p mode is $2 < E > / \tau_d \sim 5 \times 10^{22}\ {\rm ergs\ s^{-1}}$.

According to Libbrecht et al. (1986), the total energy in all the p modes (about 10^7) is 10^{34} ergs within a factor 10.

Anguera Gubau et al. (1992) and Elsworth et al. (1993) measured a global 30% decrease of the power of low degree p modes at solar maximum. This decrease seems to preclude a high value of the fraction λ of the total power which some additional source could contribute to. Nevertheless, the physical mechanisms by which the p mode power might decrease, such as damping by active regions, or modification of the properties of the convection, have not yet been quantitatively estimated. This might be

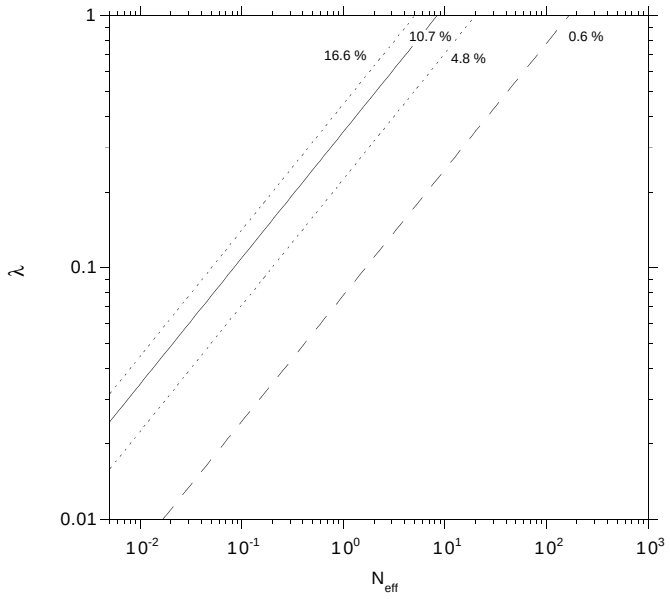

Fig. 2. Relationship between the effective number $N_{\rm eff}$ of excitations per damping time and the fraction λ of the mode power due to the secondary mechanism of excitation, in order to match the observed correlation in IPHIR and GOLF periods. The value of the correlation is indicated on each curve.

efficient enough to dominate the energy input due to an additional source. Moreover, the measurement of the amplitude of global p modes is influenced by the presence of active regions covering a significant fraction of the solar surface at solar maximum (Cacciani & Moretti, 1997). Given these uncertainties, no firm constraint can be deduced from these observations. We shall consider "likely" a fraction $\lambda \leq 30\%$.

3.3. Observed correlations

F98 determined the mean correlations between the energies of low degree p modes at two different epochs: 160 days in 1988 near solar maximum using IPHIR data ($l = 0$, $19 \leq n \leq 23$ and $l = 1$, $18 \leq n \leq 23$), and 310 days in 1996-97 near solar minimum using GOLF data ($l = 0$ and $l = 1$, $17 \leq n \leq 25$). The mean correlation coefficient $\mathcal{C}$ they measured is:

(i) $\mathcal{C} = 10.7 \pm 5.9\%$ in 1988 (IPHIR data),

(ii) $\mathcal{C} < 0.6\%$ in 1996-97 (GOLF data).

According to F98, the probability that the correlation measured from IPHIR data could occur by chance is 0.7% if the modes were independent. F98 also rejected the possibility of an instrumental artefact by checking that the noise of IPHIR data at different frequencies is not correlated.

If the granules were the only source of p-mode excitation, the correlation would be less than $10^{-5}\%$ according to Eq. (22), i.e. well below the detection limit. The actual limit of detection, of order 0.6% (F98), corresponds to at least one exciting event every 29 minutes, on average. If due to a single mechanism of excitation, the correlation measured with IPHIR data would correspond to an exciting event every 12 ± 7.2 hours.

Fig. 2 shows the relationship between $N_{\rm eff}$ and λ required by the correlations observed in IPHIR data, and the upper bound set by GOLF data.

The correlation measured by F98 in 160 days of IPHIR data imposes that $N_{\rm ad} \geq \tau_{\rm d}/160 = 0.02$ in the IPHIR period, which is coherent with the fraction of abnormal events in BiSON data. Applying Eqs. (25)-(27) to a typical mode of energy 8×10^{27} ergs and damping time $\tau_{\rm d} = 3.7$ days, the constraint $\mathcal{C} \geq 4.8\%$ leads us to look for a mechanism occurring at most a few times per day in 1988, with an acoustic energy input of at least 10^{26} ergs per mode:

$$0.02 \leq N_{\rm ad} \ \leq \ 7.1 \times \left(\frac{\beta_{\rm ad}}{4}\right)\left(\frac{\lambda}{0.3}\right)^2, \qquad (36)$$

$$< e_{\rm ad} > \ \geq \ 6.7 \times \left(\frac{4}{\beta_{\rm ad}}\right)\left(\frac{0.3}{\lambda}\right) \times 10^{26}{\rm ergs}. \qquad (37)$$

Table 1. Energy, momentum and occurrence rate of a free falling comet, a X-ray flare, and a CME (Zarro et al. 1988; Crosby et al. 1993; Hundhausen 1997)

	comet	flare	CME
kinetic energy (ergs)			
average	-	$\sim 10^{30}$	6.7×10^{30}
maximum	2×10^{32}	$\sim 10^{33}$	4×10^{32}
kurtosis β	-	~ 33	4-20
momentum (g cm s^{-1})			
average	-	$\sim 10^{22}$	$\sim 10^{23}$
maximum	6×10^{24}	-	$\sim 10^{24}$
occurrence rate (day^{-1})			
solar minimum	< 0.1	1	0.2
solar maximum	< 0.1	19	3

4. Some candidates: comet impacts, X-ray flares and coronal mass ejections

4.1. Comet impacts

Sungrazing comets of the Kreutz group are small remnants of an earlier passage of a larger progenitor comet. Among the 10 sungrazers observed by SMM, 4 appeared during the 160 days IPHIR campaign (MacQueen & St. Cyr 1991). A total of 59 sungrazers were observed by LASCO aboard SOHO. Even with an occurrence rate of 0.1 per day, $\mathcal{C} \geq 4.8\%$ in Eq. (28) would require an energy input of $6\beta_{\rm ad}^{-1/2} \times 10^{27}$ ergs per event and per mode. Given the small scale of the comet, all 10^7 p modes should receive the same energy input as low degree modes, which corresponds to a total acoustic energy of $\sim 10^{34}$ ergs per event. This already exceeds by two orders of magnitude the kinetic energy of a comet with the mass as Halley's hitting the solar surface; not to mention the variability issue between IPHIR and SOHO periods, nor the difficult question of the efficiency f of the energy transfer (addressed by Gough 1994; Kosovichev & Zharkova 1995).

4.2. X-ray flares

4.2.1. Observations of waves generated by flares

Although sunspots are known to absorb high degree acoustic waves (Braun et al. 1987, 1988), observations of the waves generated by a large solar flare on 24th April 1984 by Haber et al. (1988a,b) showed a 19% increase of power in outward travelling wave, dominating the sunspot absorption. Nevertheless, Braun & Duvall (1990) also observed the wave emission from a flare on 10th March 1989, and found an upper bound of 10% power increase, if any.

Very recently, Kosovichev & Zharkova (1998) analysed the shock wave produced by the "fairly moderate" flare of 9th July 1996, observed by MDI aboard SOHO. The wave amplitude is associated to a momentum a factor 30 smaller than the one expected from their theoretical model. This unexpectedly high efficiency led them to conclude that the seismic flare source might be located in subsurface layers.

The effect of flares on low degree modes is however less clear. The high energy events of BiSON data, appearing above the exponential energy distribution of low degree modes, do not seem to be correlated neither with the sunspot number, nor with the strength of X-ray flares (Chaplin et al. 1995). Using the sum of normalized energies of low degree modes in IPHIR data, Gavryusev & Gavryuseva (1997) found an anticorrelation between big pulses in p modes and the mean solar magnetic field but no correlation with the sunspot number.

4.2.2. Theoretical estimates of p mode excitation by flares

The theoretical estimate of the energy transmitted from a flare to p modes can follow three different approaches:

(i) the region surrounding the flare is heated and expands vertically on a time scale short enough to communicate momentum to the atmosphere below it (Wolff 1972). This process could extract 10^{28} ergs of acoustic energy from a 10^{32} ergs flare ($f \sim 10^{-4}$). According to Wolff (1972), the error bar in this estimate is at least a factor 10.

(ii) the plasma flows down towards the foot points of the field lines, and hits the solar surface, thus communicating momentum to it. This approach was followed by Kosovichev & Zharkova (1995) who found a smaller effect than that observed by Haber et al. (1988a).

(iii) the pressure perturbation associated with the restructuring of the magnetic field in the flare region might be more effective, as suggested by Kosovichev & Zharkova (1995).

4.2.3. Energy distribution of flares

The total energy released by a flare (less than 10^{27} ergs to 10^{33} ergs) is usually computed assuming that the observed hard X-rays are produced by bremsstrahlung from a distribution of accelerated electrons impinging upon a thick target plasma. Using the Hard X-Ray Burst Spectrometer on the Solar Maximum Mission satellite from 1980 to 1989, Crosby et al. (1993) showed that the flaring rate varies by about a factor 20 between the solar maximum and minimum, while the energy distribution remains constant. Applying Eq. (29) to the correlation observed by IPHIR, with the 30% variation of the p mode total power, suggests the following correlation $\mathcal{C}_{\min}$ at solar minimum:

$$0.15\% \leq \mathcal{C}_{\min} \leq 0.59\%, \tag{38}$$

which is compatible with the upper bound obtained from GOLF data.

The occurrence rate of flares follows a power law distribution $p(\mathcal{E}) \sim \mathcal{E}^{-\gamma}$ against the total flare energy with a slope $\gamma < 2$, indicating that the largest flux of energy occurs in rare big energy events. Let $\mathcal{E}_{\min} \ll \mathcal{E}_{\max}$ be the range of energies over which the power law distribution is observed, its mean energy $< \mathcal{E}_{\rm F} >$ and kurtosis $\beta_{\rm F}$ are:

$$< \mathcal{E}_{\rm F} > \sim \frac{\gamma-1}{2-\gamma} \left(\frac{\mathcal{E}_{\max}}{\mathcal{E}_{\min}} \right)^{2-\gamma} \mathcal{E}_{\min}, \tag{39}$$

$$\beta_{\rm F} \sim \frac{(2-\gamma)^2}{(3-\gamma)(\gamma-1)} \left(\frac{\mathcal{E}_{\max}}{\mathcal{E}_{\min}} \right)^{\gamma-1}. \tag{40}$$

According to Crosby et al. (1993), about 13 flares occurred per day in 1980-1982 (solar maximum), with a slope of the energy distribution $\gamma \sim 1.5$ in the range $10^{28} \leq \mathcal{E}_{\rm F} \leq 10^{32}$ ergs. Two thirds of the flares considered by Crosby et al. (1993) fall in this range according to their Fig. 6, so that the occurrence rate of these flares can be taken as 8.7 per day ($N_{\rm cme} \sim 32.2$). Eqs. (39)-(40) imply $< \mathcal{E}_{\rm F} > \sim 10^{30}$ ergs and $\beta_{\rm F} \sim 33$. Assuming that the efficiency f does not depend on the energy, the distributions of total energy and of energy input per mode are identical, and $N_{\rm eff} = 1.0$. Eqs. (25) and (33) imply:

$$22.4\% \leq \lambda \leq 44.6\% \tag{41}$$

$$< e_{\rm F} > \geq 10^{26} \text{ ergs event}^{-1} \text{ mode}^{-1}, \tag{42}$$

$$\frac{< \mathcal{E}_{\rm F} >}{< e_{\rm F} >} \leq 10^4 \text{ modes}. \tag{43}$$

With $\mathcal{E}^2 p(\mathcal{E}) \sim \mathcal{E}^{1/2}$, Eq. (32) indicates that Eq. (43) would still be correct if the energy dependence of the efficiency $f(\mathcal{E})$ were to select only the most energetic events.

The size of the flare region viewed from earth is no more than a few arcminutes, so that all p modes with a degree $l \leq l_{\max}$ must receive an equal amount of energy. With $l_{\max} = 37$ according to Wolff (1972), this corresponds to a set of $\mathcal{N} \geq 10^4$ modes, which contradicts Eq. (35). In conclusion, the total acoustic energy input required from X-ray flares to produce the observed correlation exceeds their total energy.

4.3. Coronal mass ejections

4.3.1. Geometry and timing of CMEs

Coronal mass ejections correspond to the release of 3.3×10^{15} g of matter on average, with a mean velocity of 350 km s^{-1} (SMM data from 1980 and 1984-1989, Hundhausen 1997). The footpoints of the outer loop are separated on average by about 45 degrees in latitude, i.e. much larger than an active region or flare (Harrison 1986, Hundhausen 1993). This large scale

structure favours low degree modes. According to Hundhausen (1994), the origin of the CME comes from a gradual build up and storage of energy in a pre-ejection structure (driven by the spreading of magnetic field lines, the emergence of magnetic flux, or the shear of field lines). A finite quantity of this energy is then released in a catastrophic breakdown in the stability or equilibrium of the stressed structure. When the CME is associated with an X-ray flare, the CME kinetic energy seems to be uncorrelated to the flare peak intensity (Hundhausen 1997).
In Hundhausen (1994), the acceleration of the CME observed by SMM on 23rd August, 1988 was measured. Its launching precedes the flare event (see also Harrison 1986), and the acceleration to a velocity of 1000 km s^{-1} occurs in less than 10 min (see the CMEs of 17th August, 1989 and 16th February, 1986 for similar examples in Hundhausen 1994).
Note that a CME was associated to the flare of 9th July, 1996 analysed by Kosovichev & Zharkova (1998).

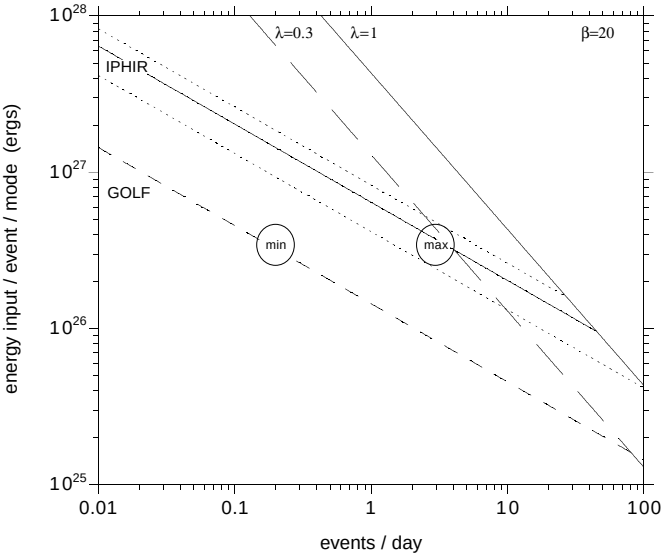

Fig. 3. Relationship between the mean acoustic energy input per mode of each impulsive event and its occurrence rate in order to produce the correlation measured from IPHIR or GOLF data. The kurtosis of the energy distribution of the source of excitation is $\beta_{\rm ad} = 20$, the energy of the mode is 8×10^{27} ergs and its damping time is $\tau_{\rm d} = 3.7$ days. The corresponding fractions of total power $\lambda = 1$ and 0.3 are indicated by the continuous and long dashed lines. The occurrence rates of CMEs at solar minimum and maximum are indicated by circles.

4.3.2. Solar cycle variability

While the average mass of a CME varies little from year to year (Hundhausen et al. 1994b), the annual variation of their mean velocity does not follow the solar cycle (Hundhausen et al. 1994a). It would therefore be interesting to check the correlation between the high energy events noticed by Chaplin et al. (1995, 1997) and this new indicator.
According to Webb & Howard (1994), the occurrence rate of CME varies from 0.2 per day at solar minimum to 3 per day at solar maximum. As for flares, the variation of the occurrence rate is enough to account for the observed variation of the correlation. Eq. (29) implies:

$$0.20\% \leq \mathcal{C}_{\rm min} \leq 3.3\%. \qquad (44)$$

4.3.3. Energy distribution of CMEs

Hundhausen et al. (1994a,b) showed that the distribution of CME velocities (10 km s^{-1} to 2000 km s^{-1}) is more widely spread than their distribution of masses (10^{14} to 10^{16} g). As a consequence, the distribution of kinetic energy is spread over a much wider range than the potential energy.
Hundhausen (1997) selected a sample of 249 CMEs measured by SMM in 1984-1989, associated with X-ray flares. The spread of their distribution of kinetic energy (from 10^{28} to 10^{33} ergs), measured from Fig. 1 of Hundhausen (1997) is such that $\beta_{\rm cme} \sim 20.2$. Note that a smaller value ($\beta_{\rm cme} \sim 3.9$) is obtained when considering the distribution of squared velocities of 109 CMEs during the 160 days IPHIR period in the catalogue of Burkepile & St. Cyr (1993). The apparent contradiction may come partly from the distribution of masses, but mostly from the high sensitivity of $\beta_{\rm cme}$ to the high energy events which occurred in 1989 at solar maximum. Moreover, fast CMEs are underrepresented in those statistics because the velocity is measured only when the CME is visible on more than one coronograph image (Hundhausen et al. 1994a). As for flares, the distribution of acoustic energy input might be different from the distribution of CMEs kinetic energy, for example, if only a subclass of CMEs excite acoustic waves. In particular, some CMEs are known to be slowly accelerated with the solar wind, while others are much faster than the solar wind (MacQueen & Fisher 1983).
With $\beta_{\rm cme} = 20$ and an occurrence rate of 3 CMEs per day ($N_{\rm cme} = 11.1$, $N_{\rm eff} = 0.6$), IPHIR correlations in Eqs. (25) and (33) imply (see Fig. 3):

$$16.7\% \leq \lambda \leq 33.2\%, \qquad (45)$$

$$< e_{\rm cme} > \geq 2.4 \times 10^{26} \text{ ergs event}^{-1} \text{ mode}^{-1}, \qquad (46)$$

$$\frac{< \mathcal{E}_{\rm cme} >}{< e_{\rm cme} >} \leq 2.8 \times 10^4 \text{ modes}. \qquad (47)$$

Estimates of both λ and the acoustic energy input per mode $< e_{\rm cme} >$ would be multiplied by a factor 2.2 if the value $\beta_{\rm cme} = 4$ were chosen. Although the kinetic energy distribution of CMEs is less accurately known than for flares, one can infer from the published ones (Hundhausen et al. 1994b, Hundhausen 1997) that the product $\mathcal{E}^2 p(\mathcal{E})$ is maximum at high energy. As for flares, Eq. (47) would not be changed if the efficiency of acoustic wave generation were highest at high energy.
Although Eqs. (45)-(47) resemble Eqs. (41)-(43) obtained for flares, the following important differences should be noted:

(i) the estimate for CMEs is based on their kinetic energy only, which is certainly much smaller than the energy of the mechanism responsible for their ejection.

(ii) the large scale of CMEs might favour the excitation of low degree modes, especially if their ejection mechanism is rooted in the convection zone ($\mathcal{N} \leq 100$).

(iii) although the range of energy of CMEs (kinetic + potential $\sim 8.5 \times 10^{30}$ ergs on average, Hundhausen et al. 1994b) is the same as for big flares, their momentum can be one hundred times larger than the momentum carried by downflowing electrons produced by flares (see Table 1). This is favourable to a higher efficiency of the energy transfer to acoustic modes.

5. Conclusion

We have investigated the consequences of interpreting the observed correlations in terms of an hypothetical excitation mechanism, in addition to the well established excitation by the granules. In particular, this interpretation requires impulsive events occurring no more than a few times per day in the IPHIR period. This has drawn our attention to the largest X-ray flares and CMEs at solar maximum. The variation of their typical energy and occurrence rate with the solar cycle could account for the variation of the correlation between the IPHIR and GOLF observations.

If due to solar flares, the correlation determined from IPHIR data requires that at least 10^{-4} of the energy of each X-ray flares is injected into each low degree mode at solar maximum. Given the number of modes (at least 10^4 due to the small scale of flares) which should receive the same energy as low degree modes, we are inclined to exclude X-ray flares regardless of the efficiency of the acoustic wave emission by each event. This reasoning, however, does not exclude the possibility of more energetic processes associated to flares, such as the restructuring of the magnetic field in the flare region mentioned by Wolf (1972) and Kosovichev & Zharkova (1995).

If the correlation is due to CMEs, at least 3.6×10^{-5} of the *kinetic* energy of each CME should be injected into each low degree mode at solar maximum. This leaves two possibilities open:

(i) CMEs may correlate only a few tens of low degree modes by injecting a few per cents of the CME kinetic energy into these modes. Higher degree modes ($l \geq 10$) would not be correlated in this case.

(ii) CMEs could correlate more modes if significantly more than the observed mechanical energy of CMEs can be extracted from their energy reservoir and injected into acoustic modes.

If all CMEs participate to acoustic emission with an efficiency f independent of their energy, they should be responsible for a fraction $16.7\% \leq \lambda \leq 33.2\%$ of low degree p mode total power at solar maximum. Nevertheless, this fraction might be significantly smaller if only a subset of high energy CMEs participates to acoustic emission. The contribution of CMEs to the low degree p mode power has to be reconciled with the observed 30% decrease of their power at solar maximum. A better theoretical understanding of the efficiency of the energy transfer from a CME event to acoustic modes is needed.

If our interpretation of IPHIR correlations is correct, we should be able to make the following observational tests:

- detect the effect of the largest CMEs on the energy of low degree p modes, even at solar minimum,
- measure the correlation $\mathcal{C}_{\min} \geq 0.2\%$ at solar minimum, using longer time series and more modes than F98,
- confirm with SOHO, during the next solar maximum, the correlations determined from IPHIR data, measure them with a better accuracy, and determine whether higher degree modes are also correlated.

Observations of the influence of CMEs on acoustic modes could improve our understanding of both the excitation of acoustic modes and the ejection mechanism of CMEs.

Acknowledgements. The author thanks T. Amari, M. Tagger, D. Gough and D. Saundby for helpful discussions.

Appendix A: energy of a mode excited stochastically

Let us consider a spherically symmetric, adiabatic model of the sun. Any perturbation of velocity v can be projected onto the basis of orthogonal eigenfunctions $\mathbf{v}_{nlm}$, associated to the (supposedly real) eigenvalues ω_{nl}. The structure of the equations allows us to write each component of the velocity vector as the product of a function of r only and a function of θ, ϕ (see e.g. Unno et al. 1989). This function is a spherical harmonic for the radial velocity v^r.

$$\mathbf{v}(\mathbf{r},t) = \sum_{nlm} A_{nlm}(t)\mathbf{v}_{nlm}(\mathbf{r}), \tag{A1}$$

$$\mathbf{v}_{nlm}(\mathbf{r}) \equiv \left[v^r_{nl}(r), v^h_{nl}(r)\frac{\partial}{\partial\theta}, v^h_{nl}(r)\frac{\partial}{\sin\theta\partial\phi}\right] Y_l^m(\theta,\phi) \tag{A2}$$

The eigenvectors are normalized as follows:

$$\int_0^{M_\star} |\mathbf{v}_{nlm}|^2 \mathrm{d}M_r = 1, \tag{A3}$$

$$= \int_0^{R_\star} \rho\left[|v^r_{nl}|^2 + l(l+1)|v^h_{nl}|^2\right] r^2 \mathrm{d}r. \tag{A4}$$

The spherical harmonics are written in terms of Legendre associated functions P_l^m:

$$Y_l^m(\theta,\phi) = (-1)^{\frac{m+|m|}{2}} q_{lm} P_l^{|m|}(\cos\theta)\mathrm{e}^{im\phi}, \tag{A5}$$

$$q_{lm} \equiv \left[\frac{2l+1}{4\pi}\frac{(l-|m|)!}{(l+|m|)!}\right]^{\frac{1}{2}}. \tag{A6}$$

The radial velocity perturbation $v_k(\mathbf{r})$ is described by Eqs. (1)-(3). The angle $\alpha \geq 0$ made by the direction θ, ϕ with the direction θ_k, ϕ_k is defined by:

$$\cos\alpha(\theta,\theta_k,\phi-\phi_k) \equiv \cos\theta\cos\theta_k + \sin\theta\sin\theta_k\cos(\phi-\phi_k). \tag{A7}$$

By projecting the perturbation onto the basis of eigenvectors, we obtain:

$$A_{nlm}(t > t_k) =$$

$$\cos\omega_{nl}(t-t_k)\int_0^{M_\star}\mathbf{v}_k(\mathbf{r})\cdot\mathbf{v}^\star_{nlm}(\mathbf{r})\mathrm{d}M_r, = \quad \text{(A8)}$$

$$2(-1)^{\frac{m+|m|}{2}}a^k_{nlm}\mathrm{e}^{-im\phi_k}\cos\omega_{nl}(t-t_k), \quad \text{(A9)}$$

$$a^k_{nlm}\equiv h^k_{nl}g^k_{lm}(\theta_k)M_k^{\frac{1}{2}}v_k \quad \text{(A10)}$$

where the real dimensionless functions $g^k_{lm}(\theta_k)$ and h^k_{nl} are defined as follows:

$$\begin{aligned} g^k_{lm}(\theta_k) &\equiv \frac{q_{lm}}{2}\int_0^{2\pi}\mathrm{d}\phi\int_0^{\pi}\mathrm{d}(\cos\theta)P_l^{|m|}(\cos\theta) \\ &\times\ \mathrm{e}^{-im(\phi-\phi_k)}g_k(\theta,\theta_k,\phi-\phi_k), \quad \text{(A11)} \\ &= q_{lm}\int_0^{\frac{\alpha_k}{2}}\mathrm{d}\phi\int_0^{\pi}\mathrm{d}(\cos\theta)P_l^{|m|}(\cos\theta) \\ &\times\ \cos(m\phi)g_k(\theta,\theta_k,\phi), \quad \text{(A12)} \\ h^k_{nl} &\equiv \frac{1}{M_k^{\frac{1}{2}}}\int_0^{R_\star}\rho r^2 v^r_{nl}(r)h_k(r)\mathrm{d}r. \quad \text{(A13)} \end{aligned}$$

Note that the function $g^k_{l,m}=g^k_{l,-m}$ is real because of the cylindrical symmetry of the impulsion.
Eq. (A9) corresponds to initial conditions with zero displacement at $t=t_k$, suitable to describe the transfer of impulsion due to a shock.
Assuming that the eigenfrequencies ω_{nl} are real, we add by hand a damping term, with a time scale τ_d. After a series of excitations indexed by k, and neglecting the transient velocities present during each event, the linearity of the equations allows us to write the velocity as follows:

$$\begin{aligned} A_{nlm}(t) &= 2(-1)^{\frac{m+|m|}{2}} \\ &\times\ \sum_{t_k<t}\mathrm{e}^{-\frac{t-t_k}{\tau_d}}a^k_{nlm}\mathrm{e}^{-im\phi_k}\cos\omega_{nl}(t-t_k). \quad \text{(A14)} \end{aligned}$$

Denoting by $\xi_{nlm}(\mathbf{r},t)$ and $\mathbf{V}_{nlm}(\mathbf{r},t)$ the displacement and velocity associated to the mode (n,l,m), the acoustic energy E_{nlm} of each mode is the sum of the kinetic and potential energies:

$$E_{nlm}\equiv\frac{1}{2}\int_0^{M_\star}(|\mathbf{V}_{nlm}|^2+\omega^2_{nl}|\xi_{nlm}|^2)\mathrm{d}M_r. \quad \text{(A15)}$$

Neglecting the slow damping compared to the fast oscillations ($\omega_{nl}\tau_d\sim 7\times10^3\gg1$ for the p modes we consider), and using the normalization (A3), we may write the energy as follows:

$$E_{nlm}(t)=\frac{1}{2}\left(|A_{nlm}|^2+\frac{1}{\omega^2_{nl}}\left|\frac{\mathrm{d}A_{nlm}}{\mathrm{d}t}\right|^2\right). \quad \text{(A16)}$$

Using Eq. (A14) and some algebra, we separate the two contributions from the waves propagating azimuthally in opposite directions:

$$E_{nlm}(t)=E^+_{nlm}(t)+E^-_{nlm}(t), \quad \text{(A17)}$$

with

$$\begin{aligned} E^+_{nlm} &\equiv \left|\sum_{t_k<t}\mathrm{e}^{-\frac{t-t_k}{\tau_d}}a^k_{nlm}\mathrm{e}^{i(\omega_{nl}t_k+m\phi_k)}\right|^2, \quad \text{(A18)} \\ E^-_{nlm} &\equiv E^+_{nl-m}. \quad \text{(A19)} \end{aligned}$$

Although Eqs. (A14) and (A16) imply $E_{nlm}=E_{nl-m}$, the two components E^+_{nlm} and E^-_{nlm}, are not equal, except on average. This separation of the components of the energy is important since the rotation enables us to separate these two components. Let us restrict ourselves to the simplest case of a solid body rotation, and neglect the Coriolis forces. This is equivalent to replacing in Eq. (A18) the azimuthal angle ϕ by $\phi+\Omega t$ and ϕ_k by $\phi_k+\Omega t_k$, and thus we obtain Eqs. (4)-(6). E^+_{nlm} is the energy associated to the frequency $\omega_{nl}+m\Omega$, while E^-_{nlm} is associated to the frequency $\omega_{nl}-m\Omega$.
The average energy input $<e_{nlm}>$ of a single random excitation onto the mode n,l,m is proportional to the total kinetic energy $\mathcal{E}$ of the perturbation:

$$<e_{nlm}>\equiv<2h^2_{nl}g^2_{lm}\mathcal{E}>. \quad \text{(A20)}$$

Appendix B: correlation produced by a single excitation mechanism

B.1. Case $N\ll1$

In order to treat the general case, we need to establish first some properties of the case $N\ll1$. The index nlm of the energy is omitted in what follows, for the sake of clarity The mean energy $<E>$ of the damped oscillator is directly proportional to the mean energy input $<e>$ of each impulsive event:

$$\begin{aligned} \frac{1}{\Delta t}\int_0^{\Delta t}(\mathrm{e}^{-\frac{t}{\tau_\mathrm{d}}})^2\mathrm{d}t &\sim \frac{N}{2}, \quad \text{(B1)} \\ <E> &\sim \frac{N}{2}<e>, \quad \text{(B2)} \\ <E^2> &\sim \frac{N}{4}<e^2>. \quad \text{(B3)} \end{aligned}$$

The energies E,E' of two modes nlm, $n'l'm'$ satisfy:

$$\frac{<EE'>}{<E><E'>}\sim\frac{1}{N}\frac{<ee'>}{<e><e'>}. \quad \text{(B4)}$$

B.2. General case

The correlation in the general case is derived using the following theorem: if a continuous function $f(x)$ satisfies $f(2x)=f(x)$ for any value of x, and $\lim_{x\to0}f(x)$ exists, then f is constant. Let us divide the random series of excitation into two independent subset of same statistical characteristics, with an occurrence rate $N/2$. Denoting by $E(N/2)$ the energy of the mode excited by only one subset, one can check from Eq. (4) that:

$$<E(N)>=2<E(N/2)>, \quad \text{(B5)}$$

and conclude that $f(N)\equiv E/N$ is a constant, which we deduce from the case $N\ll1$ (Eq. B2):

$$<E>\equiv\frac{N}{2}<e>. \quad \text{(B6)}$$

The variance of the energy can also be written as follows:

$$\frac{\mathrm{Var}\ E}{<E>^2}(N) = \frac{1}{2}\frac{\mathrm{Var}\ E}{<E>^2}(N/2) + \frac{1}{2}. \quad \text{(B7)}$$

This implies that $f(N) \equiv N(\mathrm{Var}\ E/ <E>^2 -1)$ is a constant, which we deduce from the case $N \ll 1$ (Eq. B3):

$$\frac{\mathrm{Var}\ E}{<E>^2} = 1 + \frac{1}{N}\frac{<e^2>}{<e>^2}. \quad \text{(B8)}$$

The correlation $\mathcal{C}$ between two modes nlm, $n'l'm'$ is defined as:

$$\mathcal{C} \equiv \frac{<EE'> - <E><E'>}{(\mathrm{Var}\ E)^{\frac{1}{2}}(\mathrm{Var}\ E')^{\frac{1}{2}}}. \quad \text{(B9)}$$

Using the fact that

$$\frac{<EE'>}{<E><E'>}(N) = \frac{1}{2}\frac{<EE'>}{<E><E'>}(N/2) + \frac{1}{2}, \quad \text{(B10)}$$

we conclude that $f(N) \equiv N(<EE'>/(<E><E'>) - 1)$ is a constant, which we deduce from the case $N \ll 1$ (Eq. B4). The correlation expressed by Eq. (12) is then derived from Eqs. (B8)-(B9).

Appendix C: correlation produced by two excitation mechanisms

Let us consider two independent series of impulsive events due to two different excitation mechanisms superimposed, indexed by k, characterized by the series of velocity perturbations $v_k^{(1)}, v_k^{(2)}$, and mean interpulse times $\Delta t^{(1)}, \Delta t^{(2)}$. The energy of a mode (nlm) can be decomposed into two random walks of N_1 and N_2 steps.

$$E^+_{nlm}(t) = \left| \sum_{t_k^{(1)}<t} \mathrm{e}^{-\frac{t-t_k^{(1)}}{\tau_d}} a^{k(1)}_{nlm} \mathrm{e}^{i\Phi^{k(1)}_{nlm}} + \sum_{t_k^{(2)}<t} \mathrm{e}^{-\frac{t-t_k^{(2)}}{\tau_d}} a^{k(2)}_{nlm} \mathrm{e}^{i\Phi^{k(2)}_{nlm}} \right|^2 \quad \text{(C1)}$$

Let us write this equation for two modes (nlm) and $(n'l'm')$. Hereafter we simply denote the quantities specific to the mode $(n'l'm')$ with a prime, for the sake of clarity. E_i and E'_i are the energies of the modes nlm and $n'l'm'$ excited by the excitation mechanism (i) only ($i = 1, 2$). The series of phases $\Phi^{k(1)}, \Phi^{k(2)}, \Phi^{k(1)'}, \Phi^{k(2)'}$ are independent.

$$<E> = <E_1> + <E_2>, \quad \text{(C2)}$$

$$\mathrm{Var}(E) = \mathrm{Var}(E_1) + \mathrm{Var}(E_2) + 2<E_1><E_2>, \quad \text{(C3)}$$

$$\mathrm{Var}(E)\,\mathcal{C} = \mathrm{Var}(E_1)\mathcal{C}_1 + \mathrm{Var}(E_2)\mathcal{C}_2, \quad \text{(C4)}$$

where $\mathcal{C}_i$ is the correlation between E_i and E'_i. Let us define the fractions λ, λ' of the total power of each mode contributed by the second mechanism as follows:

$$\lambda \equiv \frac{<E_2>}{<E>}, \quad \text{(C5)}$$

$$\lambda' \equiv \frac{<E_2>}{<E>}. \quad \text{(C6)}$$

Let convection be the first excitation mechanism ($C_1 = 0$), and let us use the index (ad) for the properties $N_{\mathrm{ad}}, e_{\mathrm{ad}}$ of the second excitation mechanism. Using Eqs. (B8), (12) and (C3) in (C4), we obtain:

$$\mathcal{C} = \frac{<ee'>}{<e^2>^{\frac{1}{2}}<e'^2>^{\frac{1}{2}}} \times \left(1 + \frac{N_{\mathrm{ad}}}{\lambda^2}\frac{<e>^2}{<e^2>}\right)^{-\frac{1}{2}} \left(1 + \frac{N_{\mathrm{ad}}}{\lambda'^2}\frac{<e'>^2}{<e'^2>}\right)^{-\frac{1}{2}}. \quad \text{(C7)}$$

Let $p_{\mathrm{T}}(\mathcal{E})$ be the density of probability of the additional source of energy as defined in Sect. 2.5. The number of efficient excitations per damping time is independent of f_{ad}:

$$N_{\mathrm{ad}} = N_{\mathrm{T}} \int_{\mathcal{E}_1}^{\mathcal{E}_2} p_{\mathrm{T}}(\mathcal{E})\mathrm{d}\mathcal{E}. \quad \text{(C8)}$$

The mean energy and kurtosis of the distribution of efficient events are:

$$<\mathcal{E}_{\mathrm{ad}}> = f_{\mathrm{ad}} \frac{\int_{\mathcal{E}_1}^{\mathcal{E}_2} \mathcal{E} p_{\mathrm{T}}(\mathcal{E})\mathrm{d}\mathcal{E}}{\int_{\mathcal{E}_1}^{\mathcal{E}_2} p_{\mathrm{T}}(\mathcal{E})\mathrm{d}\mathcal{E}}, \quad \text{(C9)}$$

$$\beta_{\mathrm{ad}} = \frac{\int_{\mathcal{E}_1}^{\mathcal{E}_2} p_{\mathrm{T}}(\mathcal{E})\mathrm{d}\mathcal{E} \int_{\mathcal{E}_1}^{\mathcal{E}_2} \mathcal{E}^2 p_{\mathrm{T}}(\mathcal{E})\mathrm{d}\mathcal{E}}{\left(\int_{\mathcal{E}_1}^{\mathcal{E}_2} \mathcal{E} p_{\mathrm{T}}(\mathcal{E})\mathrm{d}\mathcal{E}\right)^2}. \quad \text{(C10)}$$

The kurtosis is also independent of f_{ad}. Eq. (32) is obtained by incorporating Eqs. (C8)-(C10) into Eq. (28).

References

Anguera Gubau M., Pallé P.L., Pérez Hernández F., Régulo C., Roca Cortés T., 1992, A&A 255, 363

Appourchaux T., Gizon L., Rabello-Soares M.C., 1998, submitted to A&A

Balmforth N.J., 1992a, M.N.R.A.S. 255, 603

Balmforth N.J., 1992b, M.N.R.A.S. 255, 632

Balmforth N.J., 1992c, M.N.R.A.S. 255, 639

Baudin F., Gabriel A., Gibert D., Pallé P.L., Regulo C., 1996, A&A 311, 1024

Braun D.C., Duvall T.L. Jr, LaBonte B.J., 1987, ApJ 319, L27

Braun D.C., Duvall T.L. Jr, LaBonte B.J., 1988, ApJ 335, 1015

Braun D.C., Duvall T.L. Jr, 1990, Sol. Phys. 129, 83

Brown T.M., 1991, ApJ 371, 401

Burkepile J.T., St. Cyr O.C., 1993, NCAR Technical Notes TN-369+STR: A revised and expanded Catalogue of Mass Ejections Observed by the Solar Maximum Mission Coronograph, HAO

Cacciani A., Moretti P.F., 1997, Sol. Phys. 175, 1

Chaplin W.J., Elsworth Y., Howe R., Isaak G.R., McLeod C.P., Miller B.A., 1995, Proc. Fourth SOHO Workshop, Helioseismology, (ESA SP-376), p. 335

Chaplin W.J., Elsworth Y., Howe R., Isaak G.R., McLeod C.P., Miller B.A., New R., 1997, M.N.R.A.S. 287, 51

Chaplin W.J., Elsworth Y., Isaak G.R., Miller B.A., New R., 1998, Proc. Sixth SOHO Workshop, Structure and Dynamics of the Interior of the Sun and Sun-like Stars (ESA SP-418), in press

Crosby N.B., Aschwanden M.J., Dennis B.R., 1993, Sol. Phys. 143, 275

Elsworth Y., Howe R., Isaak G.R., McLeod C.P., Miller B.A., New R., Speake C.C., Wheeler S.J., 1993, M.N.R.A.S. 265, 888

Espagnet O., Muller R., Roudier T., Mein P., Mein N., Malherbe J.M., 1996, A&A 313, 297
Foglizzo T., García R.A., Boumier P., Charra J., Gabriel A.H., Grec G., Robillot J.M., Roca Cortés T., Turck-Chièze S., Ulrich R.K., 1998, A&A 330, 336 (F98)
Gavryusev V.G., Gavryuseva E.A., 1997, Sol. Phys. 172, 27
Goldreich P., Keeley D.A., 1977, ApJ 211, 934
Goldreich P., Kumar P., 1988, 326, 462
Goldreich P., Murray N., Kumar P., 1994, ApJ 424, 466
Goode P.R., Gough D.O., Kosovichev A.G., 1992, ApJ 387, 707
Gough D.O. 1994, M.N.R.A.S. 269, L17
Haber D.A., Toomre J., Hill F., 1988a, In: Christensen-Dalsgaard J. and Frandsen S. (eds.) Proc. IAU Symp. 123, Advances in Helio- and Astero-seismology, p. 59
Haber D.A., Toomre J., Hill F., Gough D.O., 1988b, In: Seismology of the Sun and Sun-like Stars, (ESA SP-286), p. 301
Harrison R.A., 1986, A&A 162, 283
Hundhausen A.J., 1993, J. Geophys. Res. 98, 13177
Hundhausen A.J., 1994, In: Strong K.T., Saba J.L.R., Haisch B.M., (eds.) The Many Faces of the Sun; Scientific Highlights of the Solar Maximum Mission, Springer-Verlag
Hundhausen A.J., 1997, In: Crooker N., Joselyn J. A., Feynman J. (eds.) Coronal Mass Ejections, Geophysical Monograph 99, p. 1
Hundhausen A.J., Burkepile J.T., St. Cyr O.C., 1994a, J. Geophys. Res. 99, 6543.
Hundhausen A.J., Stanger A.L., Serbicki S.A., 1994b, Proc. Third SOHO Workshop, Solar Dynamic Phenomena and Solar Wind Consequences, (ESA SP-373), p. 409
Kosovichev A.G., Zharkova V.V., 1995, Proc. Fourth SOHO Workshop, Helioseismology, (ESA SP-376), p. 341
Kosovichev A.G., Zharkova V.V., 1998, submitted to Nature
Kumar P., Franklin J., Goldreich P., 1988 ApJ 328, 879
Kumar P., Goldreich P., 1989, ApJ 342, 558
Kumar P., Lu E., 1991, ApJ 375, L35
Libbrecht K.G, Popp B.D., Kaufman J.M., Penn M.J., 1986, Nature 323, 235
MacQueen R.M., Fisher R.R., 1983, Sol. Phys. 89, 89
MacQueen R.M., St. Cyr O.C., 1991, Icarus 90, 96
Restaino S.R., Stebbins R.T., Goode P.R., 1993, ApJ 408, L57
Rimmele T.R., Goode P.R., Strous L.H., Stebbins R.T., 1995, Proc. Fourth SOHO Workshop, Helioseismology (ESA SP-376), p. 329
Unno W., Osaki Y., Ando H., Shibahashi H., 1979, In: Nonradial Oscillations of Stars, University of Tokyo Press
Vorontsov S.V., Jefferies S.M., Duval T.L. Jr., Harvey J.W., 1998, M.N.R.A.S., in press
Webb D.F., Howard R.A., 1994, J. Geophys. Res. 99, 4201
Wolff C.L., 1972, ApJ 176, 833
Zarro D.M., Canfield R.C., Strong K.T., Metcalf T.R., 1988, ApJ 324, 582